Imaging 3D Subsurface Structure at Diablo Canyon, California, Using Ambient Field Recorded by a Very Dense Array for High-Frequency Ground Motion Prediction

Report for SCEC Award #17141
Submitted November 14, 2018

Investigators: Nori Nakata (University of Oklahoma)

I. Project Overview

A. Abstract

In the box below, describe the project objectives, methodology, and results obtained and their significance. If this work is a continuation of a multi-year SCEC-funded project, please include major research findings for all previous years in the abstract. (Maximum 250 words.)

Ground-motion prediction is a key component of seismic hazard analysis, which is typically carried out using ground-motion prediction equations. To reduce the uncertainty of ground motion prediction, construction of accurate seismic velocity models is essential. The small-scale heterogeneity of the structure is used for explaining high frequency earthquake coda. In recent years, due to the technology development, portable seismic sensors (node) are available, and very dense Large-N arrays are possible to use in seismology. Due to the nuclear power plant at the Diablo Canyon and populations in the area, accurate ground motion prediction in the central California is an urgent task for seismic hazard assessment. In Diablo Canyon in the central California, Pacific Gas & Electric Company (PG&E) deployed very dense seismic sensor arrays for six weeks in 2011 and 2012, with number of sensors of 7183 and 2908, respectively. This provides a unique situation for demonstrating estimation of small-scale structural heterogeneity from the dense array and connection to the regional velocity model. I use the group velocity of Rayleigh waves to invert velocity models in the area. The tomograms show spatially high resolution and showing geologic features and similarity to active-source P-wave velocities. The high-resolution velocity structure can be used to improve small-earthquake locations, ground-motion prediction, and understanding subsurface structures.

B. SCEC Annual Science Highlights

Each year, the Science Planning Committee reviews and summarizes SCEC research accomplishments, and presents the results to the SCEC community and funding agencies. Rank (in order of preference) the sections in which you would like your project results to appear. Choose up to 3 working groups from below and re-order them according to your preference ranking.

Central California Seismic Project (CCSP)
Ground Motion Prediction (GMP)
Seismology

C. Exemplary Figure

Select one figure from your project report that best exemplifies the significance of the results. The figure may be used in the SCEC Annual Science Highlights and chosen for the cover of the Annual Meeting Proceedings Volume. In the box below, enter the figure number from the project report, figure caption and figure credits.

Figure 6. Rayleigh-wave group velocity maps at each frequency. The red and blue indicates low and high velocities, respectively. The black dots show the location of receivers.

D. SCEC Science Priorities

In the box below, please list (in rank order) the SCEC priorities this project has achieved. See *https://www.scec.org/research/priorities* for list of SCEC research priorities. *For example: 6a, 6b, 6c*

4a, 4b, 4d

E. Intellectual Merit

How does the project contribute to the overall intellectual merit of SCEC? *For example: How does the research contribute to advancing knowledge and understanding in the field and, more specifically, SCEC research objectives? To what extent has the activity developed creative and original concepts?*

Towards the physics-based ground motion prediction, subsurface velocities are important parameters. This would control the path and site effects. The central California and the Diablo Canyon area is (was) a focus area for SCEC 5, and this velocity model provides detailed velocity model with very high spatial resolution. Based on the frequencies I used (0.2—0.9 Hz), the depth sensitivity to the structure is down to 5 km. The inverted velocities have similarities to a P-wave velocity structure obtained from active seismic data. To estimate the travel time of the surface waves, I use double beamforming as an array signal processing. This double-beamforming method allows us to estimate group velocities between receiver pairs more accurately than single-station methods.

F. Broader Impacts

How does the project contribute to the broader impacts of SCEC as a whole? *For example: How well has the activity promoted or supported teaching, training, and learning at your institution or across SCEC? If your project included a SCEC intern, what was his/her contribution? How has your project broadened the participation of underrepresented groups? To what extent has the project enhanced the infrastructure for research and education (e.g., facilities, instrumentation, networks, and partnerships)? What are some possible benefits of the activity to society?*

Accurate estimation of the seismic hazard assessment is important for the Diablo Canyon area because of the nuclear power plant there. This study can contribute the ground motion modeling in this area for public safety. Also, because the cheap and user-friendly seismic sensors are becoming widely available, we can use the similar, maybe down-scaled, seismic survey to assess the seismic hazard at the area we are interested in.

G. Project Publications

All publications and presentations of the work funded must be entered in the SCEC Publications database. Log in at *http://www.scec.org/user/login* and select the Publications button to enter the SCEC Pubications System. Please either (a) update a publication record you previously submitted or (b) add new publication record(s) as needed. If you have any problems, please email *web@scec.org* for assistance.

II. Technical Report

Introduction

To reduce the uncertainty of ground motion prediction, construction of accurate seismic velocity models is essential. The small-scale heterogeneity of the structure is used for explaining high frequency earthquake coda (*Aki and Chouet*, 1975). *Restrepo-Velez and Bommer* (2003) reported that large apparent aleatory variability of ground-motion amplitudes is caused by short-wavelength heterogeneities, and the influence of these structures can become a dominant factor for seismic hazard assessment. With accurate seismic velocity models, we can better constraint path effects for each source and receiver, and hence reduce aleatory uncertainty of ground motion prediction (*Anderson and Brune*, 1999; *Atkinson*, 2006). The velocity models are used for numerical simulation of seismic wave propagation (e.g., *Olsen et al*., 1995).

Due to the nuclear power plant at the Diablo Canyon (the blue star in Figure 1) and populations in the area, accurate ground motion prediction in the central California is an urgent task for seismic hazard assessment. For the physics-based ground motion modeling of Central California Seismic Project (CCSP), estimation of seismic velocities in the region with high spatial resolution is proposed here.

For long-period ground motion, seismic tomography with regional networks is useful for mapping large-scale Earth structure, and SCEC has demonstrated the value of 3D waveform tomography for this purpose in the southern California (*Lee et al.*, 2014). For connecting seismology to civil/geophysical engineering, short-period information is necessary because the resonant frequency of such structure is much higher than the frequency we usually used for regional-scale tomography. In Diablo Canyon in the central California, Pacific Gas & Electric Company (PG&E) deployed very dense seismic sensor arrays for six weeks in 2011 and 2012 (Figure 1). Interestingly, multiple seismometers in a regional network exist in the area of the 2011 array. This provides a unique situation for demonstrating estimation of small-scale structural heterogeneity from the dense array and connection to the regional velocity model.

Geology, dataset, and ambient field

Dense arrays were deployed at Diablo Canyon, CA, in 2011 and 2012, and continuously recorded ground motion for six weeks each (Figure 1). The main structures have west-northwest trends including the Los

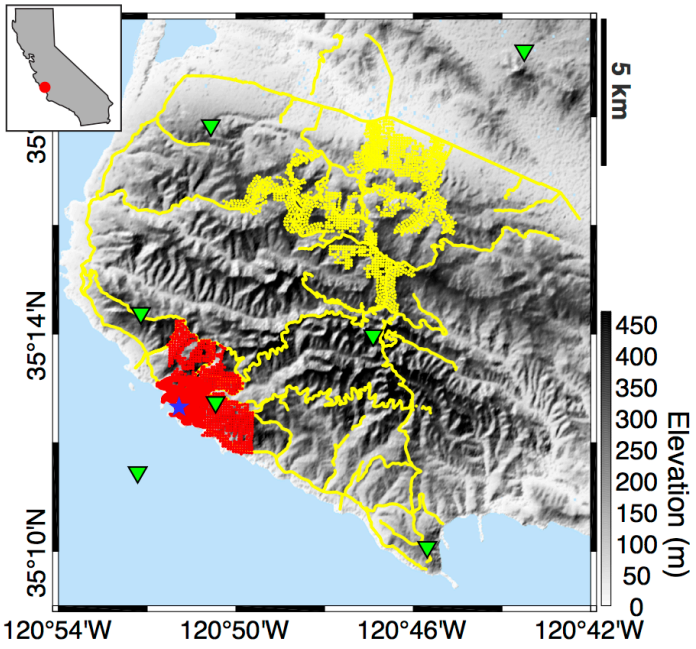

Figure 1. Receiver locations deployed at Diablo Canyon in 2011 (yellow dots) and 2012 (red dots). The green triangles are the location of PG stations (data are available at NCEDC). The blue star indicates the location of the Diablo Canyon Nuclear Power Plant. The red circle in the inset shows the location of the survey in California.

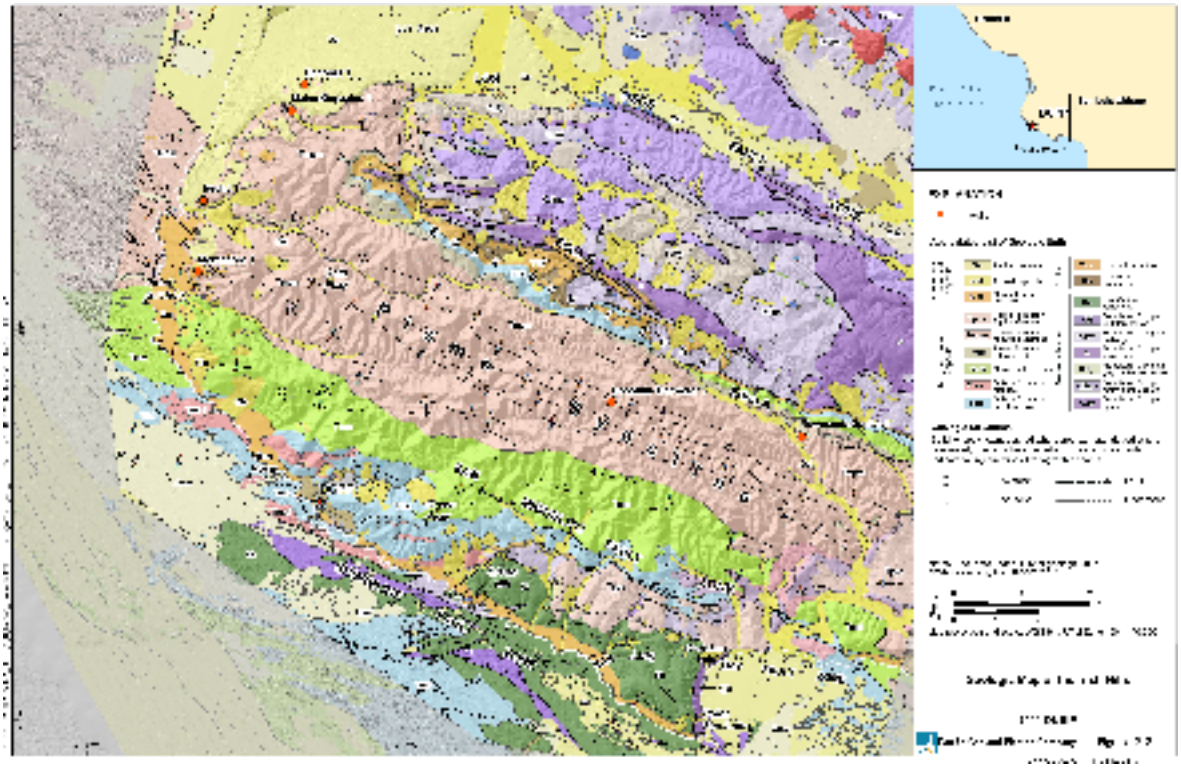

Figure 2. Surface geology map in the study area (modified after CCCSIP report (2011)).

Osos fault zone (Figure 2). The basement depth is deep (2-3 km) at the marine deposit zone (the pink in Figure 2). There is about 500-m elevation change in the array with high-wavenumber topography, which can scatter high-frequency surface and body waves (*Revenaugh*, 1995). The 2011 and 2012 arrays contain 7183 and 2908 station locations, respectively. Vertical-component 10 Hz geophones were used for continuous recording. Here, I process the continuous records in 2011. Similar to the studies of Long Beach, CA (*Lin et al.*, 2013; *Nakata et al.*, 2015), I can use the signals down to 0.25 Hz for ambient-field analyses after correcting receiver response.

The beamforming analyses (Figure 3) show that the energy of ambient field comes from variety of azi-

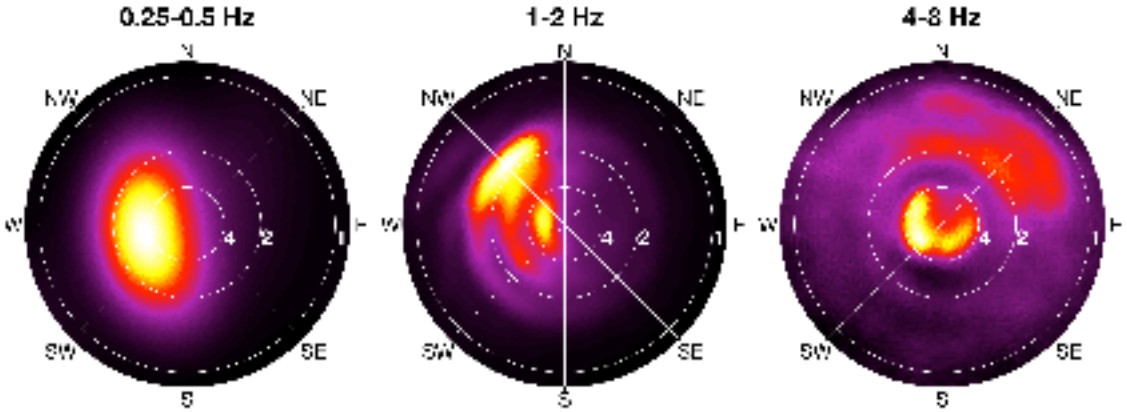

Figure 3. Power of observed ambient field at the dense 2D array (North-central part of the 2011 array) in the horizontal slowness domain after beamforming averaged over the entire six-week recording. The power is computed in three different frequency bands: 0.25-0.5, 1-2, and 4-8 Hz. Bright color indicates a direction of strong incoming energy. Power is independently normalized at each panel. The numbers at each white circle indicate the corresponding velocity in kilometers per second.

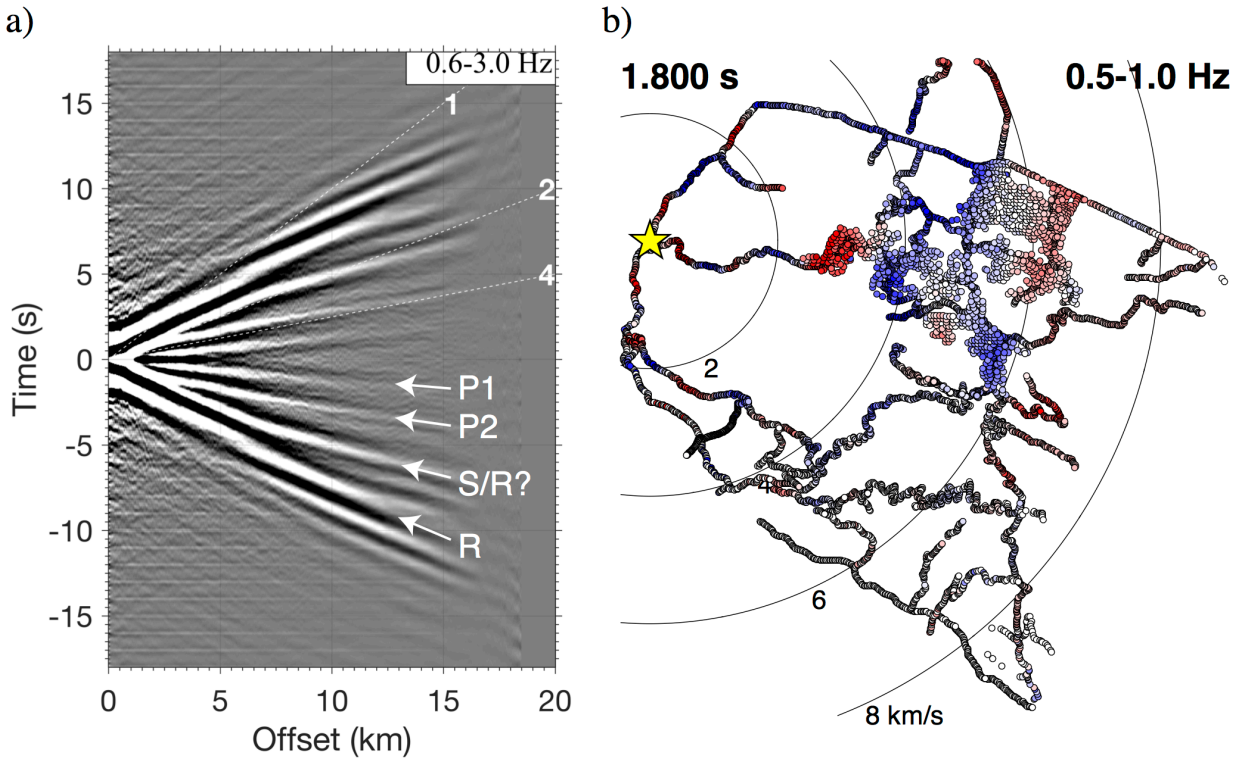

Figure 4. (a) Spatially averaged time-distance plot of crosscorrelation functions obtained from ambient field. The individual correlation waveforms (e.g., panel (b)) are averaged based on spatial bins of receiver offset, and for this average, I use all correlation functions computed (51M functions). The dashed lines indicate move-out assuming straight ray paths and constant velocity, which is shown by the white numbers. The arrows describe the interpretation of wave types, where R stands for Rayleigh wave. P1 and P2 are both P waves with different penetration depth and/or frequencies as shown in Figures 3b and 3c. (b) Snapshot of an example of individual correlation function (at 1.8 s), in which the reference receiver is shown as the yellow star. Red and blue indicate positive and negative amplitudes of waveforms, respectively. The black circles show the travel time of waves with the straight ray-path assumption.

muths probably because the arrays are surrounded by the coast, and ambient field is mainly related to

the oceanic waves especially for lower frequencies. With reciprocity, if the ambient field comes from greater than 180 degrees, I can extract accurate Green's function in any directions (*Wapenaar and Fokkema*, 2006). In lower frequencies, Rayleigh waves are dominantly observed (Figure 3). The velocity of 3~3.5 km/s is about the velocity of the crust (0.25-0.5 Hz), and in higher frequencies, the Rayleigh waves become slower as expected. Instead, the strong energy is observed with much faster velocities (4-8 Hz; 4~6 km/s), which is the energy of P waves. The high-frequency energy in the NE direction might be related to the cultural noise at San Luis Obispo.

Ambient field tomography

With the 2011 array, I compute crosscorrelation functions between all receiver pairs (about 51 million pairs). I follow the stacking approach proposed by *Nakata et al*. (2015) to increase the signal-to-noise ratio (SNR). Due to the number of receivers and ambient-field source distribution, binned-stacked correlation gather in Figure 4a shows clear traveling waves in multiple wave types. The bin size is 200 m. I interpret that these waves are mainly P and Rayleigh waves because I use vertical-component geophones. To identify these waves, detail analyses are required. Surface waves are clearly constructed even from individual correlation functions (Figure 4b). For this frequency range, the rough topography (Figure 1) does

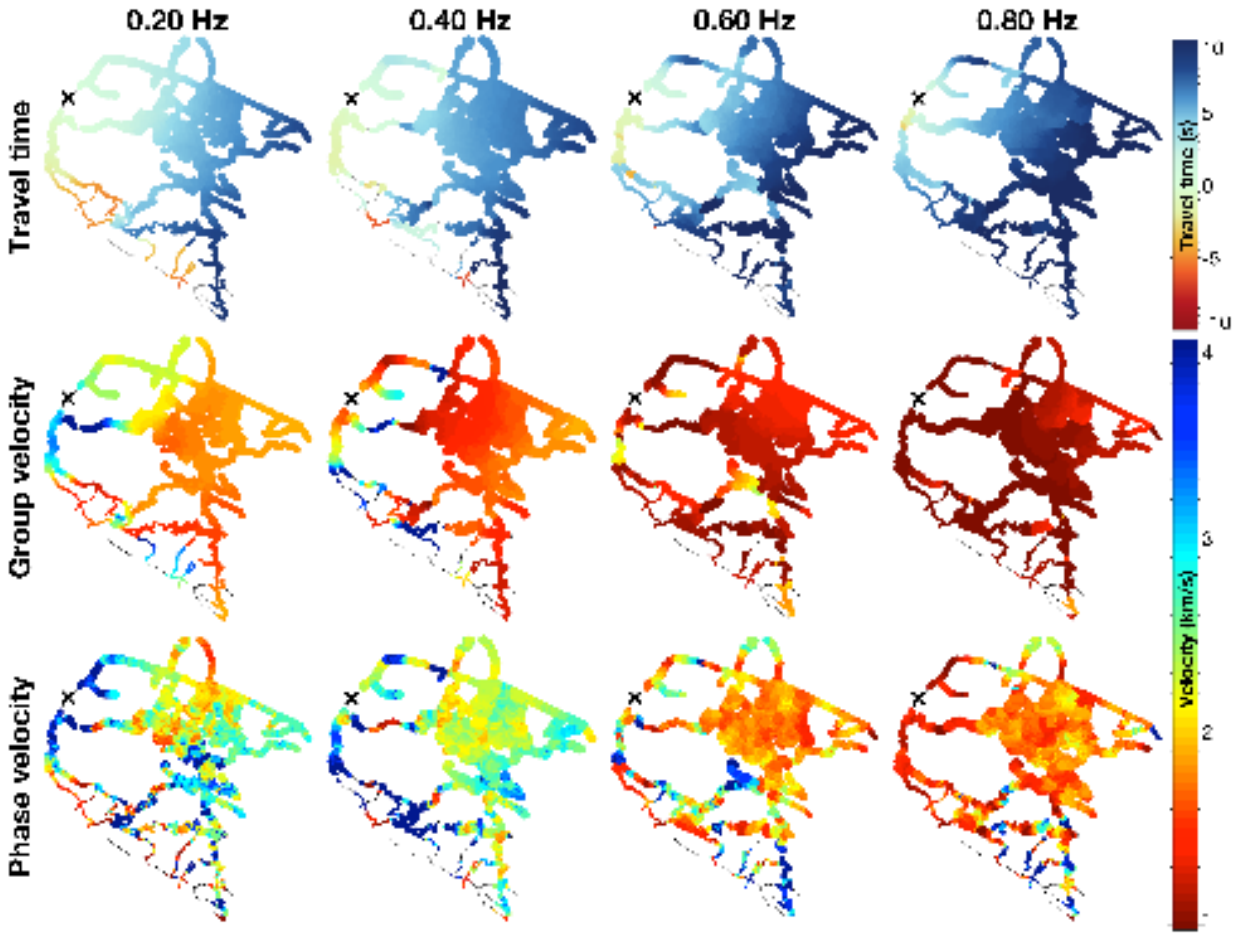

Figure 5. An example estimation of travel time, group and phase velocities at different frequencies. The black cross shows the location of the center of the source array, and colored dots show the centers of the receiver array.

not significantly disturb the spatial coherency of wavefields. Although P waves are not as clear as surface waves in each correlation, SNR will be increased by applying advanced signal processing techniques (*Nakata et al.*, 2015; *Nakata et al.*, 2016), and then I can apply the body-wave tomography using the extracted P waves, which is a future work.

To enhance signal-to-noise ratio of Rayleigh waves in Figure 4 and estimate group velocities between receiver pairs, I apply double beamforming (*Nakata et al*., 2016; *Roux et al.,* 2016). Double beamforming (DBF) is an array-based signal processing technique to identify or extract waves based on slowness and azimuth as similar to the single beamforming shown in Figure 3, but between two arrays. I discretize the array space into 100x100 grids, and apply DBF between each grid to extract direct-path Rayleigh waves. After the DBF, because the wavefields are in the slowness domain with higher signal-to-noise ratio compared to the original data, I can estimate the phase and group velocities between two points (Figure 5). These points are the center of the two arrays used.

After DBF, I obtain group velocity measurements between all possible grid pairs. Then I apply a group velocity tomography method (*Barmin et al.,* 2001) to invert velocities at each frequency (Figure 6). This tomography is 2D inversion, because I run inversion separately between each frequency. The WNW-ESE geology tread is recovered well, and also low-frequency velocities are higher, as expected. The spatial resolution is about 0.01 degree. Based on the residual analyses (Figure 7), the tomography inversion reduces the residuals significantly. The initial model is homogeneous velocities for 1.4 km/s, and we iterate 10 times with changing smoothing factors. Note that the velocity structure estimated from the Group velocity is similar to the P-wave velocities obtained from active-source travel-time tomography (PGEQ report, 2013).

Conclusions

We use the continuous seismic record with the densely-sampled geophone array (7200 stations) at Diablo Canyon to image the subsurface velocity structure. The tomograms show spatially high resolution and showing geologic features and similarity to active-source P-wave velocities. The high-resoultion velocity structure can be used to improve small-earthquake locations, ground-motion prediction, and understanding subsurface structures.

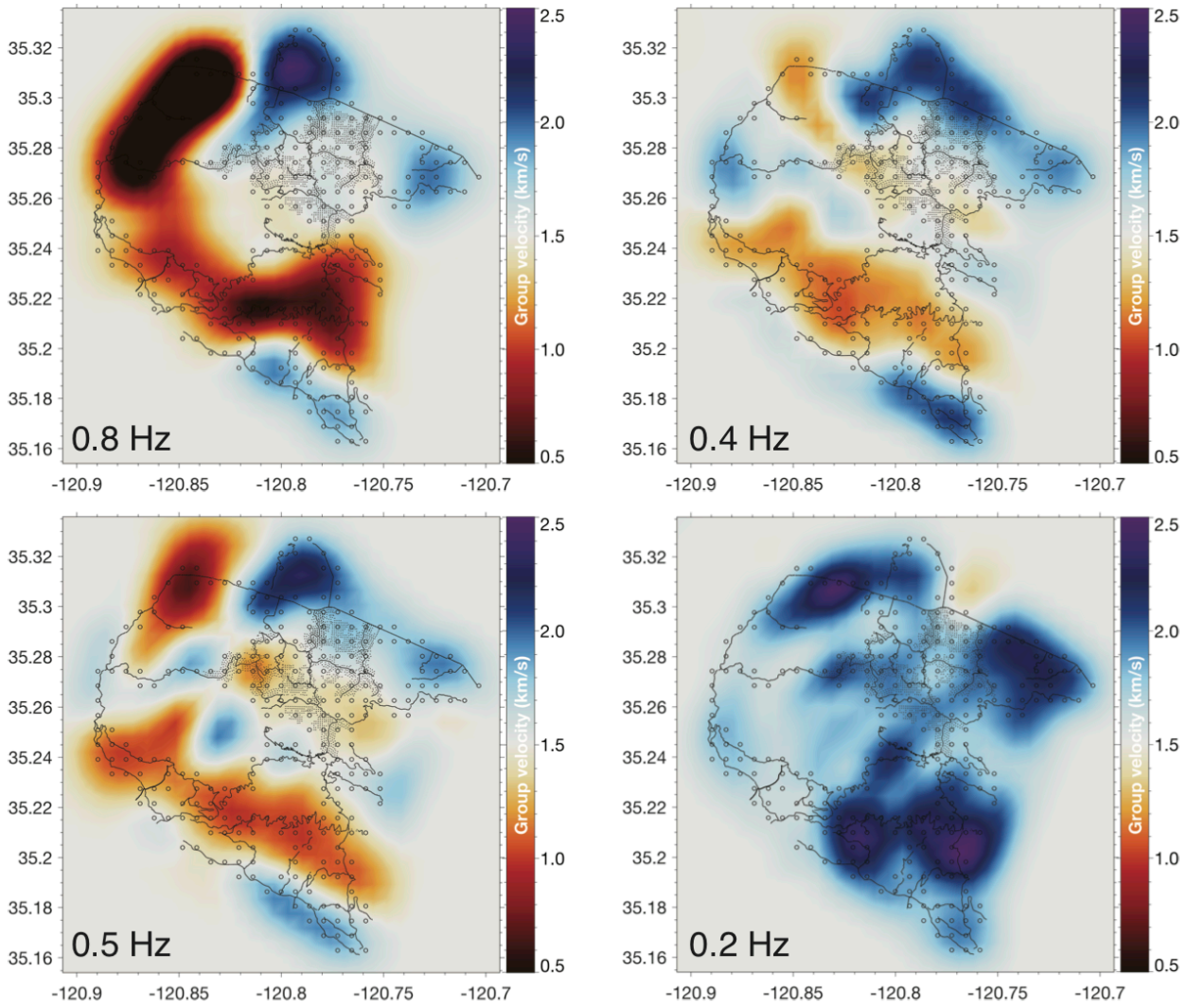

Figure 6. Rayleigh-wave group velocity maps at each frequency. The red and blue indicates low and high velocities, respectively. The black dots show the location of receivers.

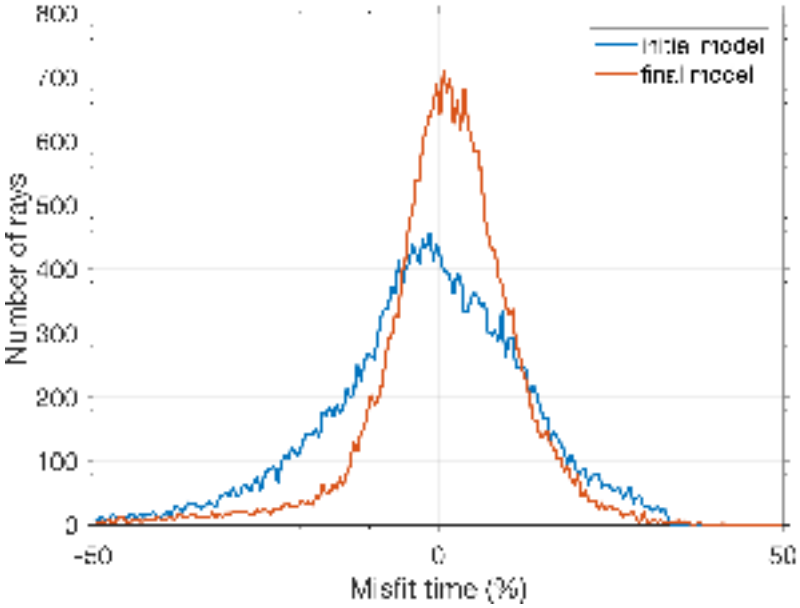

Figure 7. Data misfits for the initial and final models in 0.4 Hz.

References

Aki, K. and B. Chouet (1975) Origin of coda waves: Source, attenuation, and scattering effects, *J. Geophys. Res.,* **70**(23), 3322-3342.

Anderson, J. G. and J. N. Brune (1999) Probabilistic seismic hazard analysis without the ergodic assumption, *Seismol. Res. Lett.*, **70**, 19-28.

Atkinson, G. M. (2006) Single-station sigma, *Bull. Seismo. Soc. Am.*, **96**(2), 446-455.

Barmin, M. P., M. H. Ritzwoller, and A. L. Levshin (2001) A fast and reliable method for surface wave tomography, *Pure appl. Geophys*. **158**, 1351-1375.

Lee, E-. J., P. Chen, T. H. Jordan, P. B. Maechling, M. A. M. Denolle, and G. C. Beroza (2014) Full 3-D tomography for crustal structure in Southern California based on the scattering-integral and the adjoint-wavefield methods, *J. Geophys. Res.*, **119**(8), 6421-6451.

Lin, F-. C., D. Li, R. W. Clayton, and D. Hollis (2013) High-resolution 3D shallow crustal structure in Long Beach, California: Application of ambient noise tomography on a dense seismic array, *Geophysics*, **78**(4), Q45-Q56.

Nakata, N. and G. C. Beroza (2015) Stochastic characterization of mesoscale seismic velocity heterogeneity in Long Beach, California, *Geophys. J. Int.,* **203**, 2049-2054.

Nakata, N., P. Boue, F. Brenguier, P. Roux, V. Ferrazzini, and M. Campillo (2016) Body and surface wave reconstruction from seismic noise correlations between arrays at Piton de la Fournaise volcano, *Geophys. Res. Lett.,* **43**, 1047-1054.

Olsen, K. B., J. C. Pechmann, and G. T. Schuster (1995) Simulation of 3D elastic wave propagation in the Salt Lake Basin, *Bull. Seism. Soc. Am.,* **85**(6), 1688-1710.

Restrepo-Velez, L. F. and J. J. Bommer (2003) An exploration of the nature of the scatter in ground motion prediction equations and the implications for seismic hazard assessment, *J. Earthquake Eng.,* **7**(S1), 171-199.

Revenaugh, J. (1995) The contribution of topographic scattering to teleseismic coda in Southern California, *Geophys. Res. Lett.*, **22**(5), 543-546.

Roux, P., L. Moreau, A. Lecointre, G. Hillers, M. Campillo, Y. Ben-Zion, D. Zigone, and F. Vernon (2016) A methodological approach towards high-resolution surface wave imaging of the San Jacinto Fault Zone using ambient-noise recordings at a spatially dense array, *Geophys. J. Int.*, **206**, 980-992.